E2-2001-206

G.N.Afanasiev[1], V.G.Kartavenko, J.Ruzicka[2]

PECULIARITIES OF CHERENKOV RADIATION IN DISPERSIVE MEDIA

Submitted to «Physica B»

[1]E-mail: afanasev@thsun1.jinr.ru
[2]Faculty of Mathematics and Physics, Comenius University, 84215, Bratislava, Slovakia

1 Introduction

In 1937, Tamm and Frank have obtained electromagnetic field (EMF)strengths of a charge uniformly moving in medium in an ω representation [1]. They found that this charge should radiate mainly at the angle defined by

$$\cos\theta_c = nc/v, \tag{1.1}$$

where c is the light velocity in vacuum, v is the charge velocity and n is the medium refractive index. However, Tamm and Frank did not consider a particular form of the medium dispersion law. This step was made by Fermi [2] who approximated the dielectric permittivity by the one-pole formula

$$\epsilon = 1 + \frac{\omega_L^2}{\omega_0^2 - \omega^2 + ip\omega}. \tag{1.2}$$

broadly used for the description of optical phenomena (see, e.g., [3,4]). Fermi noted that since n in the above definition of the Cherenkov angle θ_c depends on ω, there is a chance that the r.h.s. of the equation defining $\cos\theta_c$ will be smaller than 1. For the dielectric permittivity chosen by Fermi, there are always ω satisfying the above condition and, therefore, the charge moving uniformly in medium with the one-pole parametrization of dielectric permittivity should radiate at each velocity. This conclusion was not made by Fermi himself, but it inevitably follows from his consideration. Further, Fermi did not consider the space-time structure of the induced EMF and the frequency distribution of the emitted radiation.

This gap was filled in a number of papers where the space-time distribution of the radiated energy was investigated analytically and numerically. It was found in [5] the EMF of a charge uniformly moving in a medium without damping described by (1.2) with $p = 0$. It was shown there that the distribution of the radiated energy crucially depended on the fact whether the charge velocity is greater or smaller than some critical velocity c_0 coinciding with the medium light velocity at small frequencies. For $v > c_0$, the radiation presents a relatively thin bunch of peaks attached to a moving charge and concentrated near the angle θ_0 defined by $\cos\theta_0 = c_0/v$. For $v < c_0$, the radiation is confined to the cone, the vertex of which is not attached to a moving charge, but lies at some distance behind it. As the charge velocity diminishes, this distance increases, while the solution angle of the above cone decreases. In Refs. [6], the radiation of a charge uniformly moving in medium with ϵ given by (1.2) (which includes damping) was considered. It was shown that the distribution of EMF intensity was highly sensitive to the value of a damping parameter p. However, calculations made in [5,6] had a serious drawback: they did not relate the frequency region to which the major part of the evaluated energy distribution was confined with the experimentally observed frequency region. Partly this drawback was overcome in [7], where the Cherenkov radiation of relativistic $v \sim c$ charges moving in air was studied. However, the results

of these investigations had a rather limited range of applicability. The reason is that in Cherenkov experiments with gases (see, e.g.,[8]), the refractive index was changed by varying gas pressure. Since the refractive index of the air under the atmospheric pressure only slightly differs from unity, it is impossible to reach conditions under which the charge velocity will be well below the Cherenkov threshold.

The aim of this consideration is to remove some of these insufficiencies. When evaluating a particular space-time distribution of the radiated energy, we analyse its frequency distribution to be sure that it lies in the observed frequency region. We apply this analysis to particular substances for which the parametrization of ϵ is known. The first substance is iodine for which the parametrization of ϵ may be found in the Brillouin book [9]. Its resonance frequency lies in a far ultra-violet region and ϵ tends to 1 for $\omega \to \infty$. In this case there is a critical velocity below and above of which the properties of radiation differ appreciably. The other substance is ZnSe for which the parametrization of ϵ may be found in [10]. Its resonance frequency lies in a far infra-red region and ϵ tends to the constant value for $\omega \to \infty$. There are two critical velocities for this case. The behaviour of radiation is essentially different above the large critical velocity, between smaller and larger critical velocities and below the smaller critical velocity. Despite the fact that the parametrization (1.2) is valid in a rather narrow frequency region, we apply it to the whole ω semi-axis. Since we deal mainly with frequency distributions of radiation, we can at any step to limit consideration to the suitable frequency region.

The plan of our exposition is as follows.
In section 2, we find distributions of radiation on the surface of a cylinder coaxial with the motion axis for different values of the charge velocity and damping parameter p, and supply main analytical formulae needed for numerical calculations. In section 3, we find frequency distributions of the radiation found in the previous section. New analytic formulae are obtained for the position of frequency regions to which radiation is confined in the presence of dispersion. The analytic results are obtained by numerical calculations. If ω_0 in (1.2) is chosen in a standard way, then the above radiation distributions being applied to iodine (for which the parameters entering into (1.2) are known) will be confined to the Roentgen region. Section 4 is devoted to the analysis of the recent experiment [10] in which the Cherenkov radiation arising from the electric dipoles moving in ZnSE crystal was observed below the Cherenkov threshold. With the same medium parameters as in [10], we evaluated frequency distribution of the radiated energy for the point-like charges moving in ZnSe. The are two critical velocities in this case. Again, new analytical formulae defining the position of frequency regions to which the radiation is confined are obtained. We discuss complications with the observation of the radiation below the Cherenkov threshold. In section 5, we apply considerations of the previous section to the experiment with electric dipoles [10]. Alternative reasons for the radiation observed in [10] below the Cherenkov threshold are discussed. Section 6 summarizes main results obtained.

2 Distribution of radiation on the cylinder surface

We choose the dielectric permittivity in the form (1.2). The EMF strengths corresponding to this permittivity on the surface of a cylinder of the radius ρ coaxial with the motion axis are given by [5,6]

$$H_\phi(\vec{r},t)=\frac{2e}{\pi v c}\int\limits_0^\infty \omega d\omega (a^2+b^2)^{1/4}[\cos(\frac{\phi}{2}+\alpha)K_{1r}-\sin(\frac{\phi}{2}+\alpha)K_{1i}],$$

$$E_z(\vec{r},t)=-\frac{2}{\pi v^2}\int\limits_0^\infty \omega d\omega\{[\cos\alpha(\epsilon_r^{-1}-\beta^2)-\sin\alpha\epsilon_i^{-1}]K_{0i}+[\sin\alpha(\epsilon_r^{-1}-\beta^2)+\cos\alpha\epsilon_i^{-1}]K_{0r}\},$$

$$E_\rho(\vec{r},t)=\frac{2}{\pi v^2}\int\limits_0^\infty \omega d\omega (a^2+b^2)^{1/4}[(\epsilon_r^{-1}\cos\alpha-\epsilon_i^{-1}\sin\alpha)(\cos\frac{\phi}{2}K_{1r}-\sin\frac{\phi}{2}K_{1i})-$$

$$-(\epsilon_i^{-1}\cos\alpha+\epsilon_r^{-1}\sin\alpha)(\sin\frac{\phi}{2}K_{1r}+\cos\frac{\phi}{2}K_{1i})]. \qquad (2.1)$$

Here $\alpha=\omega(t-z/v)$, v is a charge velocity,

$$K_{0r}=ReK_0(\frac{\rho\omega}{v}\sqrt{1-\beta^2\epsilon}),\quad K_{0i}=ImK_0(\frac{\rho\omega}{v}\sqrt{1-\beta^2\epsilon}),$$

$$K_{1r}=ReK_1(\frac{\rho\omega}{v}\sqrt{1-\beta^2\epsilon}),\quad K_{1i}=ImK_1(\frac{\rho\omega}{v}\sqrt{1-\beta^2\epsilon}),$$

ϵ_r and ϵ_i are real and imaginary parts of ϵ:

$$\epsilon=\epsilon_r+i\epsilon_i,\quad \epsilon_r=1+\frac{\omega_L^2(\omega_0^2-\omega^2)}{(\omega_0^2-\omega^2)^2+p^2\omega^2},\quad \epsilon_i=-\frac{p\omega\omega_L^2}{(\omega_0^2-\omega^2)^2+p^2\omega^2},$$

$$\epsilon_r^{-1}=\epsilon_r/(\epsilon_r^2+\epsilon_i^2),\quad \epsilon_i^{-1}=-\epsilon_i/(\epsilon_r^2+\epsilon_i^2).$$

Further,

$$1-\beta^2\epsilon=a+ib,\qquad a=1-\beta^2\epsilon_r,\quad b=-\beta^2\epsilon_i. \qquad (2.2)$$

We need also to write out explicitly $\sqrt{1-\beta^2\epsilon}$ entering into these expressions. Its sign should be chosen in such a way as to guarantee the decrease of EMF strengths at large distances. This gives

$$\sqrt{1-\beta^2\epsilon}=(a^2+b^2)^{1/4}(\cos\frac{\phi}{2}+i\sin\frac{\phi}{2}),$$

$$\cos\frac{\phi}{2}=\frac{1}{\sqrt{2}}(1+\frac{a}{\sqrt{a^2+b^2}})^{1/2},\quad \sin\frac{\phi}{2}=\frac{1}{\sqrt{2}}(1-\frac{a}{\sqrt{a^2+b^2}})^{1/2}. \qquad (2.3)$$

The radial Poynting vector

$$S_\rho=\frac{c}{4\pi}(\vec{E}\times\vec{H})_\rho=-\frac{c}{4\pi}E_zH_\phi$$

measures the energy flux per unit of time through the unit surface element of the cylinder surface. Therefore, $S_\rho = d^2\mathcal{E}/dSdt$, where $dS = \rho dz d\phi$. Then,

$$\sigma_\rho = 2\pi\rho S_\rho = d^2\mathcal{E}/dzdt \tag{2.4}$$

is the energy flowing per unit of time through the ring of the radius ρ with a unit length along the z axis.

The energy flux per unit length through the surface of the cylinder of the radius ρ coaxial with the z axis for the whole time of charge motion is defined by

$$W = \int_{-\infty}^{+\infty} \sigma_\rho dt = \frac{1}{v}\int_{-\infty}^{+\infty} \sigma_\rho dz, \tag{2.5}$$

$$\sigma_\rho = 2\pi\rho S_\rho, \quad S_\rho = \frac{c}{4\pi}(\vec{E}\times\vec{H})_\rho = -\frac{c}{4\pi}E_z H_\phi.$$

2.1 Application to iodine

As an example, we consider the dielectric medium with : $\epsilon_0 = 1 + \omega_L^2/\omega_0^2 \approx 3$, $p/\omega_0 \approx 0.015$. The parameters of this medium are close to those given by Brillouin ([10], p. 56) for iodine. As to ω_0, Brillouin recommends $\omega_0 \approx 4\cdot 10^{16} sec^{-1}$. This value of ω_0 approximately 10 times larger than the average frequency of the visible region. However, since all formulae used for calculatons depend only on the ratios ω_L/ω_0 and p/ω_0, we prefer to fix ω_0 only at the final stage.

In Figs 1-5, we present the distributions of dimensionless radial energy fluxes $\tilde{\sigma}_\rho = \sigma_\rho/(e^2\omega_0^3/c^2)$ on the surface of the cylinder coaxial with the motion axis for different charge velocities. Theory predicts [5,6] that in the absence of damping ($p = 0$) and for the ρ fixed, σ_ρ as a function of $z - vt$ should oscillate behind the moving charge) with the period $\pi v/\omega_0$. To estimate the influence of the imaginary part of dielectric permittivity, we give radial energy fluxes for $p/\omega_0 = 10^{-6}$, $p/\omega_0 = 0.015$ and $p/\omega_0 = 0.15$ (Brilloin recommends the last value).

What can we learn from these figures?

1) For $\beta < \beta_c$, the increase in p leads to a much more stronger decrease in the energy fluxes than for $\beta > \beta_c$ (compare Figs.1 and 2 with Figs. 4 and 5). Here $\beta_c = 1/\sqrt{\epsilon_0}$ is the light velocity in medium for small frequencies.

2) With increasing p, the tails of radial energy fluxes decrease much stronger than their maxima (compare a, b, c parts of Figs. 1-5).

It should be mentioned that in Figs. 1-5 the intensities are presented as a function of dimensionless variable $\tilde{z} = \omega_0(z - vt)/c$. According to [6], the period of intensity oscillations is π/β in these units.

3 Frequency distribution of radiation

Substituting E_z and H_ϕ given by (2.2) into (2.5) and integrating over the whole time motion t one presents W in the form

$$W = \int_0^\infty f(\omega)d\omega,$$

where

$$f(\omega) = -\frac{2e^2\rho}{\pi v^3}\omega^2(a^2+b^2)^{1/4}\{(K_{0r}K_{1r}+K_{0i}K_{1i})[(\epsilon_r^{-1}-\beta^2)\sin\frac{\phi}{2}-\epsilon_i^{-1}\cos\frac{\phi}{2}]-$$

$$-(K_{0i}K_{1r}-K_{0r}K_{1i})[(\epsilon_r^{-1}-\beta^2)\cos\frac{\phi}{2}+\epsilon_i^{-1}\sin\frac{\phi}{2}]\} \qquad (3.1)$$

describes the frequency distribution of the radiated energy.

Consider now the limit $p \to 0$. Let $1-\beta^2\epsilon > 0$ in this limit, then

$$\sin\frac{\phi}{2} \to 0,\ \cos\frac{\phi}{2} \to 1,\ \epsilon_i \to 0,\ \epsilon_i^{-1} \to 0,\ K_{0i} \to 0,\ K_{1i} \to 0$$

and, therefore, $f(\omega) \to 0$. On the other hand, if in this limit $1-\beta^2\epsilon < 0$, then:

$$\sin\frac{\phi}{2} \to 1, \quad \cos\frac{\phi}{2} \to 0,\ \epsilon_i \to 0,\ \epsilon_i^{-1} \to 0,$$

$$K_{0r} \to -\frac{\pi}{2}N_0,\ K_{0i} \to -\frac{\pi}{2}J_0,\ K_{1r} \to -\frac{\pi}{2}J_1,\ K_{1i} \to \frac{\pi}{2}N_1,$$

where the argument of the Bessel functions is $\rho\frac{|\omega|}{v}\sqrt{|1-\beta^2\epsilon|}$. Substituting this into (3.1) and using the relation

$$J_\nu(x)N_{\nu+1}(x) - N_\nu(x)J_{\nu+1}(x) = -\frac{2}{\pi x}$$

one arrives at

$$f(\omega) = \frac{e^2\omega}{c^2}(1-\frac{1}{\epsilon\beta^2}). \qquad (3.2)$$

This in turn leads to W exactly coinciding with the Tamm-Frank formula.

3.1 Conditions for the appearance of radiation

Obviously, the non-damping behaviour of EMF is possible when the real part of $\sqrt{1-\beta^2\epsilon}$ is small (otherwise, K_0 and K_1 functions defining EMFs will be infinitely small at large observation distances and, therefore there will be no radiation). For this, it should be

$$a = 1-\beta^2\epsilon_r < 0, \quad \text{and} \quad b << |a|.$$

It is convenient to operate with dimensionless variables

$$\omega \to \omega/\omega_0, \quad p \to p/\omega_0, \quad \omega_L \to \omega_L/\omega_0.$$

Then,

$$\epsilon_r = 1 + \frac{\omega_L^2(1-\omega^2)}{(1-\omega^2)^2 + p^2\omega^2}, \quad \epsilon_i = -\frac{p\omega\omega_L^2}{(1-\omega^2)^2 + p^2\omega^2},$$

$$1 - \beta^2\epsilon = a + ib,$$

$$a = 1 - \beta^2\epsilon_r, \quad b = \beta^2\epsilon_i.$$

We need also the frequency regions where $1 - \beta^2\epsilon_r > 0$ and $1 - \beta^2\epsilon_r < 0$.
Let

$$\beta_c < \beta < 1, \quad \beta_c = 1/\epsilon_0, \quad \epsilon_0 = \epsilon(0) = 1 + \omega_L^2.$$

Then, $1 - \beta^2\epsilon_r < 0$ for $0 < \omega^2 < \omega_1^2$ and $1 - \beta^2\epsilon_r > 0$ for $\omega^2 > \omega_1^2$, where

$$\omega_{1,2}^2 = 1 \pm \Omega_0 - \frac{1}{2}(p^2 + \beta^2\gamma^2\omega_L^2), \quad \Omega_0 = [\frac{1}{4}(p^2 + \beta^2\gamma^2\omega_L^2)^2 - p^2]^{1/2}.$$

In particular, $\omega_1 = 1$ for $\beta = 1$ and $\omega_1 = \sqrt{1-p^2}$, $\omega_2 = 0$ for $\beta = \beta_c$.
Let

$$\beta_p^2 < \beta^2 < \beta_c^2,$$

where

$$\beta_p^2 = \frac{2p - p^2}{\omega_L^2 + 2p - p^2}$$

(it is therefore suggested that p is sufficiently small to guarantee the positivity of β_p^2. This is always fulfilled for transparent media where the Cherenkov radiation is observed). Then, $1 - \beta^2\epsilon_r < 0$ for $\omega_2^2 < \omega^2 < \omega_1^2$ and $1 - \beta^2\epsilon_r > 0$ for $\omega^2 < \omega_2^2$ and $\omega^2 > \omega_1^2$.
In particular, $\omega_1 = \omega_2 = \sqrt{1-p}$ for $\beta = \beta_p$.
Let

$$0 < \beta < \beta_p.$$

Then, $1 - \beta^2\epsilon_r > 0$ for all ω and there is no room for $1 - \beta^2\epsilon_r < 0$.

We see that for $\beta > \beta_c$, the frequency distribution of the radiation differs from zero for $0 < \omega < \omega_1$, while for $\beta_p < \beta < \beta_c$ it is confined to the frequency window $\omega_2 < \omega < \omega_1$. Further decrease in β leads to the window narrowing. The window width disappears for $\beta = \beta_p$ when $\omega_1 = \omega_2 = \sqrt{1-p}$.

Now, the oscillatory behaviour of EMF strengths in addition to $1 - \beta^2\epsilon_r < 0$ requires also $b << |a|$. This gives

$$\omega_L^2 \frac{\omega p - 1 + \omega^2}{(1-\omega^2)^2 + p^2\omega^2} << 1 - \frac{1}{\beta^2}$$

(it was taken into account that $1-\beta^2\epsilon_r<0$). Since the r.h.s. of this inequality is smaller than 0, its l.h.s. should also be smaller than 0. This takes place if

$$\omega<\sqrt{1+p^2/4}-p/2.$$

For small damping this reduces to $\omega<1-p/2$. These conditions for the appearance of radiation are new and, as far as we know, have not been obtained previously.
To illustrate the afore-said, we present in Figs. 6 and 7 dimensionless spectral distributions $\tilde{f}(\omega)=f(\omega)/(e^2\omega_0/c^2)$ for different charge velocities β and damping parameters p as a function of dimensionless frequency $\tilde{\omega}=\omega/\omega_0$.
The parameter ϵ_0 was chosen to be 9 (as for iodine), so that $\beta_c=1/\sqrt{\epsilon_0}=1/3$. For $\beta_p<\beta<\beta_c$, one observes that $f(\omega)$ is confined to the frequency window $\omega_2<\omega<\omega_1$ (Figs. 6, a, b). For $\beta\to\beta_p$ the window width tends to 0.

For $\beta=\beta_c$, $\omega_2=0$, $\omega_1=\sqrt{1-p^2}$ and $f(\omega)$ fills the frequency region $0<\omega<\sqrt{1-p^2}$ (Fig.6 c). For $\beta\to 1$, ω_1 tends to 1 and $f(\omega)$ is confined to the region $0<\omega<\omega_1$ (Figs. 7 a and b).

Turning to the dependences of spectral distributions from the value of the damping parameter p, one observes that for $\beta<\beta_c$, dependences $f(\omega)$ are more sensitive to the decrease in p than for $\beta>\beta_c$. Compare, e.g., Figs. 6a and 7b. From Fig. 7b ($\beta=0.8$) one sees that an increase in p from 10^{-6} to 10^{-2} leads to the decrease in $f(\omega)$ by 2.5 times. On the other hand, the same increasing of p for $\beta=0.2$ (Fig. 6a) results in an almost complete disappearance of $f(\omega)$.

So far, we did not specified the resonance frequency ω_0. If, following Brillouin [10], we choose $\omega_0=4\cdot 10^{16}sec^{-1}$ (which is approximately 10 times larger than average frequency of the visible light), then it follows from Fig. 6 that for $\beta<\beta_c$ frequency distributions are practically zero inside the region of the visible light corresponding to $\omega\approx 0.1$. This means, in particular, that space-time distributions of the radiated energy shown in Figs. 1-5 are formed mainly by photons lying in the Roentgen domain and, therefore, there is no chance to observe them in the region of visible light.

Another support for this claim is to consider the well-known Cherenkov shock wave arising from a charge motion in an infinite non-dispersive medium with penetrability ϵ. For simplicity, we limit ourselves to the vector potential. For $\beta>\sqrt{\epsilon}$ it is given by the following integral:

$$A_z=\frac{e}{c}\int_0^\infty d\omega\{\sin[\omega(t-z/v)]J_0-\cos[\omega(t-z/v)]N_0\}.$$

Here J_0 and N_0 are Bessel and Neumann functions of the argument $\sqrt{\beta^2\epsilon-1}\omega\rho/v$. The integration over ω gives

$$A_z=\frac{2e\beta}{[(vt-z)^2-(\beta^2\epsilon-1)\rho^2]^{1/2}}\Theta(vt-z-\rho\sqrt{\beta^2\epsilon-1}). \qquad (3.3)$$

The presence of the Θ function guarantees that A_z differs from zero only inside the Cherenkov cone the vertex of which coincides with the current position of a charge. It is easy to see that A_z is infinite on the surface of the Cherenkov cone. The frequency distribution corresponding to the motion in an infinite nondispersive medium is given by (3.2) in which ω runs from 0 to ∞. This means that all the frequencies give contribution to the Cherenkov shock wave (3.3).
From this viewpoint, the most promising substance for the observation of radiation for $\beta < \beta_c$, seems to be the usual water which has a narrow transparency region between two absortion ones (see, e.g., [11]. However, we have not found any parametrization of its dielectric permittivity in the rather broad frequency region in the physical literature. For the water, the parametrization of ϵ should have at least two resonance frequencies.

4 Spectral analysis of the Cherenkov radiation in ZnSe

Recently, we have been aware of an experiment [10] which seems to support predictions made in [5,6]. The experiment was performed on a single ZnSe crystal of the cubic form with a side 5 mm. Its refractive index essentially differs from unity in the physically interesting region. A lazer pulse from an external source is injected into the sample. This laser pulse represents a wave-packet centered around the frequency ω_L which may be varied in some interval. The injected pulse propagating with a group velocity defined by ω_L creates the distribution of electric dipoles following the laser pulse. The moving dipoles produce EMF, the properties of which depend on the dipole velocity v_d which, in its turn, is defined by ω_L. In particular, this velocity can be greater or smaller than some critical velocity c_0 depending on the substance properties. In the treated experiment, the measured quantity was the electric field. The character of observed time oscillations crucially depended on the fact whether $v_d > c_0$ or $v_d < c_0$. According to [10], the observed time oscillations were in good agreement with theoretical ones predicted in [5,6]. In Ref. [10], the following parametrization of a dielectric permittivity was chosen:

$$\epsilon = \epsilon_\infty + \frac{\omega_L^2}{\omega_0^2 - \omega^2} \tag{4.1}$$

with

$$\epsilon_\infty = \epsilon(\omega = \infty) = 5.79, \quad \epsilon_0 = \epsilon(\omega = 0) = \epsilon_\infty + \frac{\omega_L^2}{\omega_0^2} = 8.64,$$

$$\omega_0 = 2\pi\nu_0, \quad \nu_0 = 6.3 \times 10^{12} Hz, \quad \omega_0 \approx 4 \cdot 10^{13} sec^{-1}.$$

There is an important difference between parametrizations (1.2) and (4.1). It is seen that $\epsilon(\omega)$ given by (1.2) tends to unity for $\omega \to \infty$. This means that medium oscillators have not enough time to be excited in this limit. On the other hand, $\epsilon(\omega)$

given by (4.1) tends to ϵ_∞ in the same limit. This leads to the appearance of two critical velocities (see below).
Now we evaluate the frequency distribution of the energy radiated by a point-like charge uniformly moving in ZnSe with the same parameters as in [10]. Certainly, the radiation of the point-like electric charge is not the same as that of the electric dipoles layer. However, the analysis of the frequency spectrum produced by the the point-like electric charge recovers the complications with the observation of the radiation below the Cherenkov threshold. We believe that these considerations can be applied to the experiment [10] with electric dipoles moving in ZnSe.
For the parametrizations (4.1), the radiation ($1 - \beta^2\epsilon < 0$) and non-radiation ($1 - \beta^2\epsilon > 0$) conditions are fulfilled in the following ω domains:

For the charge velocity greater than the larger critical velocity ($\beta > \beta_\infty, \quad \beta_\infty = 1/\sqrt{\epsilon_\infty} \approx 0.416$) the radiation condition $1 - \beta^2\epsilon < 0$ takes place if $0 < \omega^2 < 1$ and $\omega^2 > \omega_1^2$. Here $\omega_1^2 = 1 + (\beta^2\epsilon_0 - 1)/(\beta^2\epsilon_\infty - 1)$. There is no radiation if $1 - \beta^2\epsilon > 0$. This is realized if $1 < \omega^2 < \omega_1^2$. For the charge velocity between two critical velocities ($\beta_0 < \beta < \beta_\infty, \quad \beta_0 = 1/\sqrt{\epsilon_0} \approx 0.34$), the radiation condition $1 - \beta^2\epsilon < 0$ takes place if $0 < \omega^2 < 1$. and $\omega^2 > \omega_1^2$. There is no radiation if $1 - \beta^2\epsilon > 0$. This is realized if $\omega^2 > 1$ Finally, for the charge velocity smaller than the minor critical velocity ($0 < \beta < \beta_0$), the radiation condition $1 - \beta^2\epsilon < 0$ is realized in the frequency window $\omega_1^2 < \omega^2 < 1$. There is no radiation outside this window (that is, for $0 < \omega^2 < \omega_1^2$ and $\omega^2 > 1$.

We summarize: for $\beta > \beta_\infty$, the frequency distribution is confined to the following ω regions: $0 < \omega^2 < 1$ and $\omega^2 > \omega_1^2$. This is demonstrated in Fig. 8, where the frequency distributions are shown for different velocities $\beta > \beta_\infty$ and different values of the damping parameter p. We observe that an increase in p by 10^5 times (from 10^{-6} to 10^{-1}) only slightly changes $f(\omega)$. In the region between two thresholds ($\beta_0 < \beta < \beta_\infty$), $f(\omega)$ differs from zero in the interval $0 < \omega < 1$ (Fig. 9 a). Increase in p from 10^{-6} to 10^{-1} changes $f(\omega)$ approximately by 10 times. Below the second threshold ($\beta < \beta_0$), $f(\omega)$ is confined to the interval $\omega_1 < \omega < 1$. When β diminishes, ω_1 tends to 1 and the available interval becomes narrower (Fig. 9, b, c). The increase in p affects $f(\omega)$ much stronger than in former cases. These conditions defining frequency region to which the radiation is confined are new and, as far as we know, have never been obtained previously.

Now, the experiments described in [10] were performed in particular, for the charge velocity $\beta = 0.3$, that is well below the minor critical velocity ($\beta = 0.34$). If the particles moving in ZnSe were the point-like charges, then, the frequency distribution shown in Fig. 9 b should be observed.

Taking for the observed frequency $\nu = 3 \cdot 10^{12} Hz$ or $\omega \approx 1.9 \cdot 10^{13} sec^{-1}$ (the electric field with this frequency was observed in [10]), then, $\omega/\omega_0 \approx 0.5$. Turning to Fig. 9b, we see that this ω lies outside the frequency region where $f(\omega) \neq 0$ even for the very small unrealistic $p/\omega_0 = 10^{-6}$.

According to [12], the finite dimensions of a moving charge lead to the cut-off of

the frequency spectrum approximately at $\omega_c = v/a$, where v is the charge velocity and a is its dimension. If for a we take the width of the electric dipoles layer realized in [10] ($a = 10^{-3}cm$), then we get $\omega_c = 6 \cdot 10^{12}sec^{-1}$ for $\beta = 0.2$ (below the minor critical velocity) $\omega_c = 1.2 \cdot 10^{12}sec^{-1}$ for $\beta = 0.4$ (between the minor and larger critical velocities) and $\omega_c = 2.4 \cdot 10^{12}sec^{-1}$ for $\beta = 0.8$ (above the larger critical velocity). For the velocity $\beta = 0.3$ (coinciding with the velocity of electric dipoles layer observed in [10]), $\omega_c = 9 \cdot 10^{12}sec^{-1}$. Therefore, $\omega_c/\omega_0 \approx 0.2$. Turning to Fig. 9,b, we see that the maximal available frequency lies at the left of radiation intensities curves (and outside them). Situation becomes still worse, if for a we take the radius of the electric dipole layer (which is much larger than its width). Therefore, if the experiment described in [10] were performed with electric charges (not electric dipoles), it could hardly give information on the existence of Cherenkov radiation below the minor threshold. Although the calculations for electric charges are not the same as for electric dipoles, they may shed some light on the critical points related to the observation of radiation below the Cherenkov threshold.
In general, Fig.9 specifies the frequency region where the observations should be made in order to discover the radiation below the Cherenkov threshold. For example, Fig. 9b tells us that for $\beta = 0.3$ and $p = 10^{-2}$ the maximum of the radiation intensity is approximately at $\omega/\omega_0 = 0.85$. For smaller damping parameter this maximum shifts to $\omega/\omega_0 = 1$.

5 Discussion

In a previous section, we analyzed the properties of the radiation generated by a point-like charge uniformly moving in $ZnSE$. But the experiment described in [10] was performed with electric dipoles. Previously, the radiation of point-like electric dipole moving in dispersive medium was considered by Frank [13, 14] who shown that the frequency distribution of the radiation equals 0 for $\beta n < 1$. For $\beta n > 1$ it equals

$$f_{\|}(\omega) = \frac{\omega^3 \mu p^2}{c^2 v^2}(1 - \frac{1}{\beta^2 n^2}) \tag{5.1}$$

for the electric dipole oriented along the velocity and

$$f_{\perp}(\omega) = \frac{\omega^3 \mu n^2 p^2}{2c^4}(1 - \frac{1}{\beta^2 n^2})^2 \tag{5.2}$$

for the electric dipole perpendicular to the velocity. Here p is the electric dipole moment, ϵ and μ are electric and magnetic penetrabilities of the medium. The space-time distribution of the emitted radiation for the electric dipole moving in nondispersive medium was obtained in [15]. Comparing (5.1) and (5.2) with the frequency distribution of a moving point-like charge

$$f_e(\omega) = \frac{\omega}{c^2}(1 - \frac{1}{\beta^2 n^2}), \quad \beta n > 1$$

we observe their similarity. Therefore, all complications with the observation of the radiation produced by a point-like charge below the Cherenkov threshold, take place also for the moving point-like electric dipole. However, experiment described in [10] was performed with a moving layer consisting of electric dipoles. The consideration of the previous section shows that the spectral analysis of the emitted radiation is of the paramount importance. This was not made in [10] (and it is in progress now). We briefly enumerate the possible alternative reasons for the radiation observed in [10]:
1) A bunch of electric dipoles is created at one side of the ZnSe cube and propagates towards the other. Such finite motion corresponds to the so-called Tamm problem (see, e.g., [16]), describing the charge motion on a finite interval. Theory [1, 16] and experiment [8, 17, 18] predict that a charge uniformly moving in a finite dielectric slab radiates at each velocity even in the absence of dispersion. This assertion is not changed by the fact that, in the treated experiment, the wavelength is much smaller than the motion interval (equal to the side of the cube);
2) As we have seen in Sect. 3, the switching on the imaginary part of dielectric permittivity leads to the damping of EMF oscillations for $v < c_0$ and to their rather small attenuation for $v > c_0$. For the realistic imaginary parts, the oscillations for $v < c_0$ are almost washed out. Unfortunately, there is no information in [10] either about the value of the imaginary part of dielectric permittivity.
3) An important question is the distance at which the observations were made: angular oscillations of EMF's intensity sharply different from the Cherenkov ones and extending far beyond the Cherenkov angular region appear at finite observation distances [19, 20];
4) Theory predicts that observation results crucially depend on the fact whether the observation time is smaller or greater than the motion time [19].

The treated experiment is so important and fundamental that any ambiguity in its interpretation should be excluded. Careful analysis of the influence of items 1)-4) on the treated experiment should be made.

6 Conclusion

We briefly summarize the main results obtained:
Previously obtained [6] analytic formulae for the radiation intensity are applied to particular substances, iodine and ZnSE, with quite different dielectric properties and for which parameterizations of dielectric permittivity are known. The influence of the charge velocity and the damping parameter on the radiation intensities is investigated. Frequency regions to which the radiation is confined are determined for the medium with dispersion. It turns that there is one critical velocity for iodine. Below and above this velocity, a moving charge radiates in a different way. There are two critical velocities for ZnSe.These considerations are applied to the recent

intriguing experiment [10] where the radiation of the electric dipoles moving in ZnSe was observed below the Cherenkov threshold. With the same ZnSe parameters as in [10], we evaluated spectral distributions of the radiated energy for the moving point like charges. The complications with the observation of radiation below the Cherenkov threshold are discussed. Probably, these considerations are applicable to the experiment with electric dipoles [10]. The alternative reasons for the radiation observed in [10] below the Cherenkov threshold are pointed out.

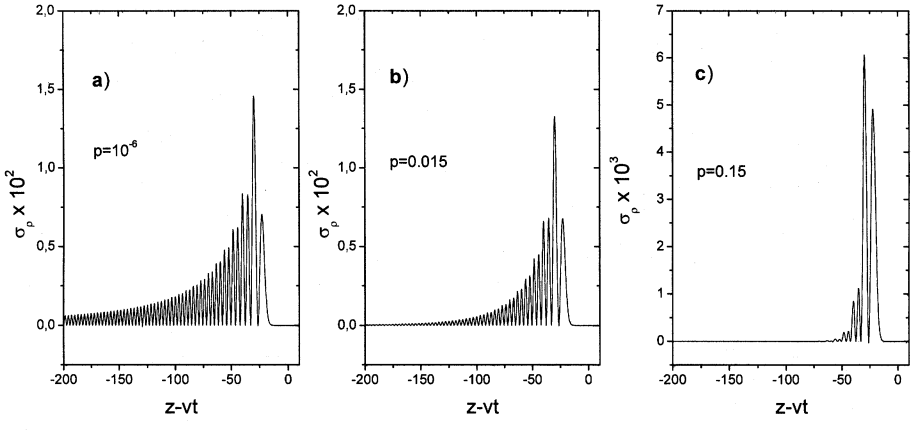

Fig.1: Dimensionless distributions of the energy radiated per unit length in the radial direction on the surface of a cylinder of the radius $\rho = 10$ (in units c/ω_0) for the charge velocity $\beta = 0.8$ and damping parameters $p = 10^{-6}$ (a), $p = 0.015$ (b) and $p = 0.15$ (c). The critical velocity $\beta_c = 1/3$; $(z - vt)$ is in units c/ω_0. It is seen that increase in p affects mainly the tails of distributions.

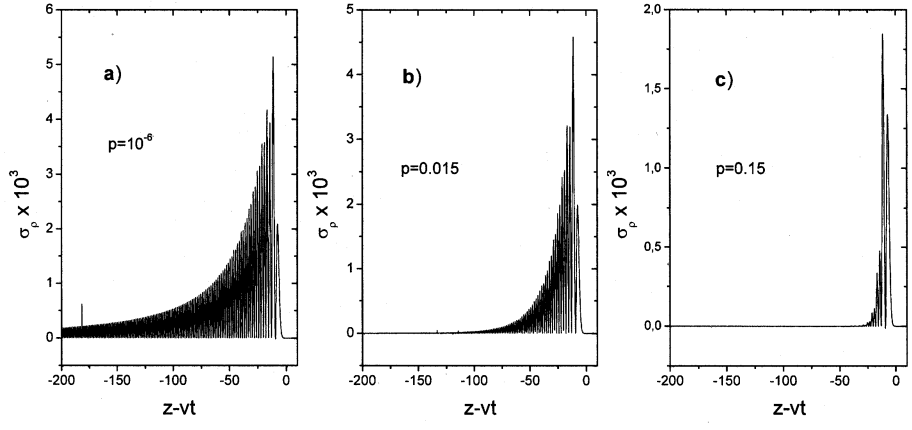

Figure 2: The same as in Fig.1, but for the charge velocity $\beta = 0.4$.

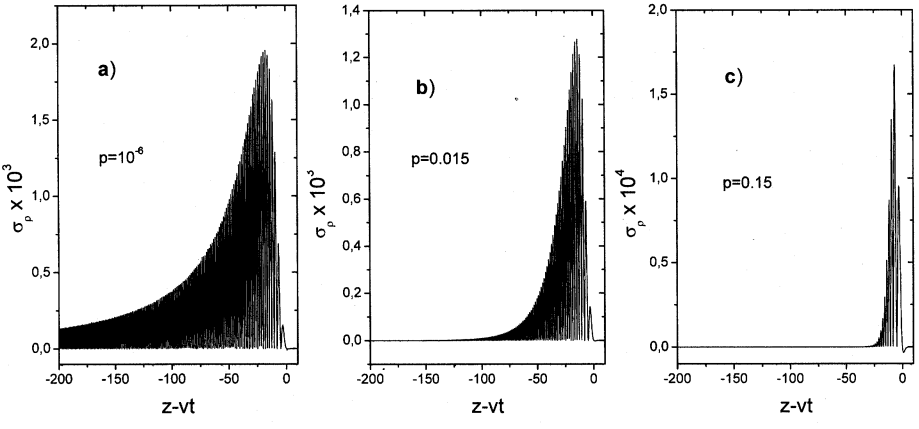

Fig.3: The same as in Fig.1, but for the charge velocity $\beta = 1/3$ coinciding with the critical velocity.

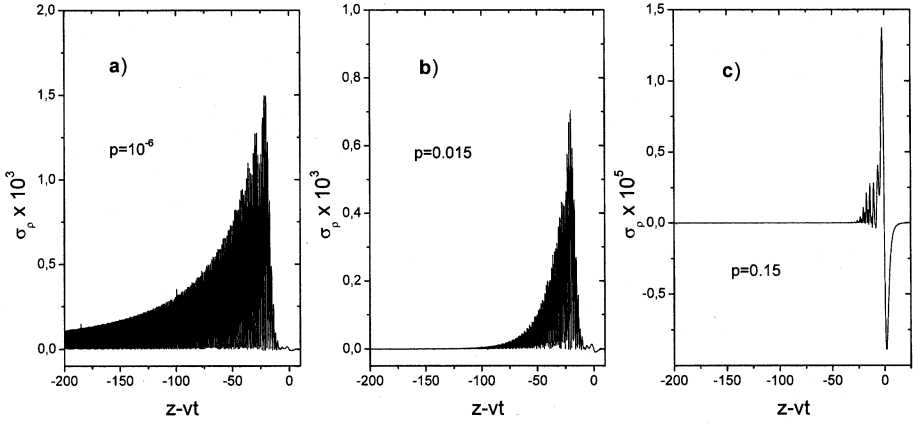

Fig.4: The same as in Fig.1, but for the charge velocity $\beta = 0.3$ slightly below the critical velocity. The characteristic oscillation near $z = vt$ corresponds to the non-radiating part of the energy flux (it is the energy flux that a charge carries with itself).

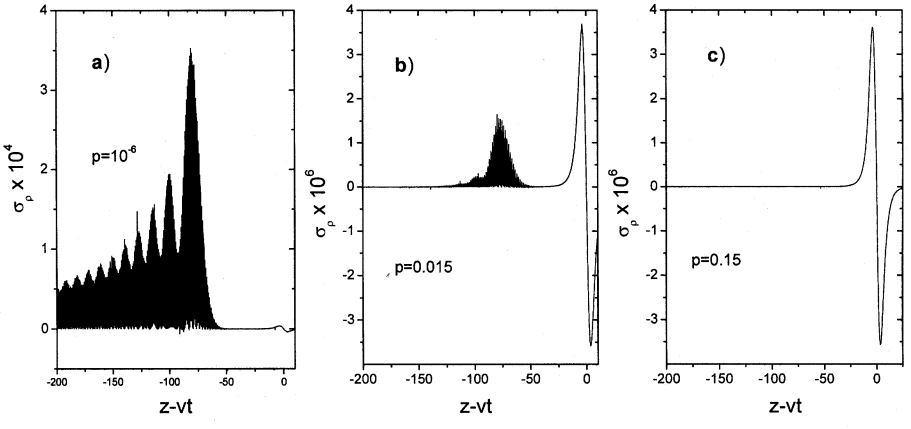

Fig.5: The same as in Fig.4, but for the charge velocity $\beta = 0.2$ well below β_c. It is seen that increase in p leads to the complete disappearance of oscillations behind the moving charge.

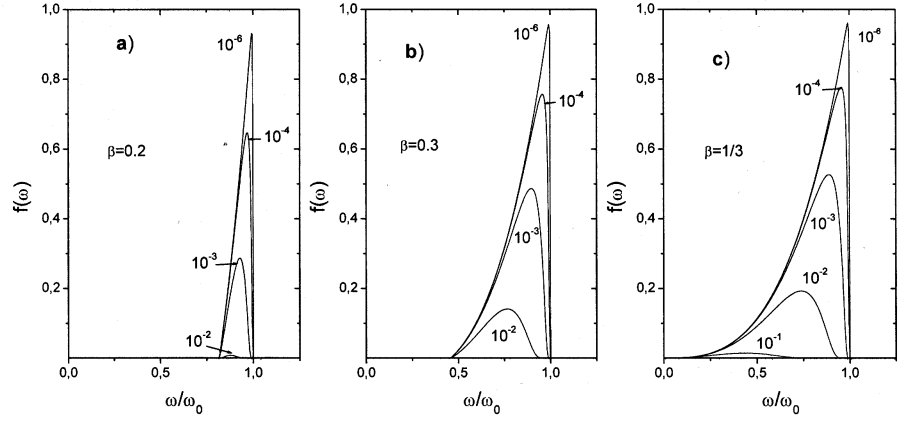

Fig.6: Dimensionless spectral distributions of the energy radiated per unit length in the radial direction for the charge velocities below ($\beta = 0.2$ (a), $\beta = 0.3$ (b)) and equal ($\beta = 1/3$ (c)) to the critical velocity. Numbers at curves mean damping parameters p; ω is in units of ω_0. We observe that increase in p strongly affects $f(\omega)$.

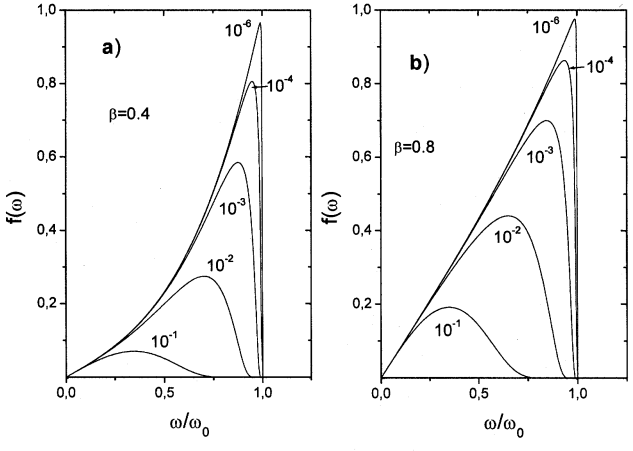

Fig.7: The same as in Fig.6, but for the charge velocities ($\beta = 0.4$ (a) and $\beta = 0.8$ (b)) above the critical velocity. It is seen that $f(\omega)$ are not so sensitive to the decrease in p as for $\beta \leq \beta_c$.

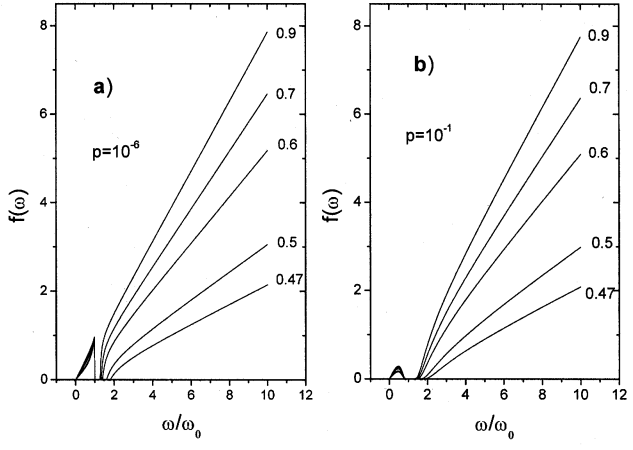

Fig.8: Dimensionless spectral distributions of the energy radiated per unit length in the radial direction for the damping parameters $p = 10^{-6}$ (a) and $p = 10^{-1}$ (b). These frequency distributions should be observed in $ZnSE$ crystall used in [10]. Numbers at curves mean β which in this figure are greater than the larger critical velocity $\beta_\infty = 0.416$. ω is in units of ω_0. It is seen that increase in p by 10^5 times only slightly changes $f(\omega)$.

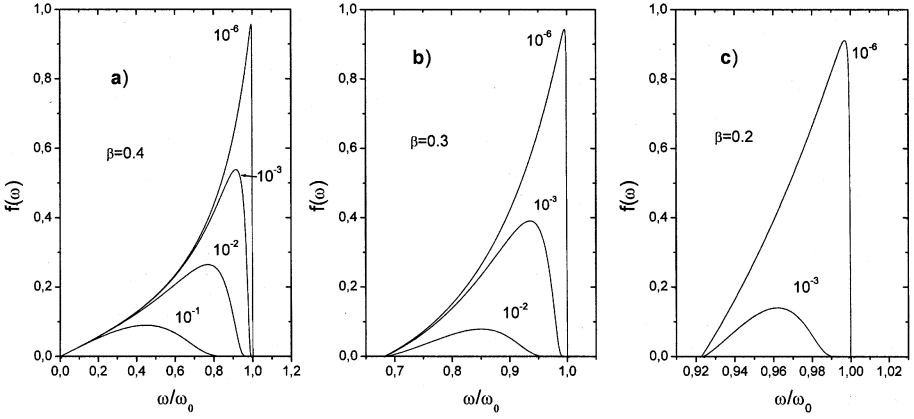

Fig.9: Dimensionless spectral distributions of the energy radiated per unit length in the radial direction for the charge velocities between the critical velocities $\beta_0 \approx 0.34$ and $\beta_\infty = 0.416$ (a) and below β_0 (b and c). Numbers at curves mean damping parameters p. It is seen that $f(\omega)$ are much more sensitive (especially, for $\beta < \beta_0$) to the change of p than for $\beta > \beta_\infty$.

References

[1] Frank I.M., 1988, *Vavilov-Cherenkov Radiation* (Moscow, Nauka), in Russian.

[2] Fermi E., 1940, Phys. Rev., **57**, 485.

[3] Born M. and Wolf E., 1975, *Principles of Optics*, (Oxford, Pergamon);

[4] Landau L.D. and Lifshitz E.M, 1992, *Electrodynamics of Continuous Media*, (Moscow, Nauka), in Russian.

[5] Afanasiev G.N., Kartavenko V.G., 1998, J. Phys. D, 31, 2760; Afanasiev G.N., Eliseev S.M, Stepanovsky Yu.P.,1999, Physica Scripta, 60, 535;

[6] Afanasiev G.N., Kartavenko V.G., Magar E.N., 1999, Physica B 269, 95; Afanasiev G.N., Kartavenko V.G., 1999, Izv. RAN., ser. fiz., 63, 5;

[7] Kartavenko V.G., Afanasiev G.N. and Greiner W., 1999, Physica B 271, 192.

[8] Aitken D.K. et al., 1963, Proc. Phys. Soc. 82, 710.

[9] Brillouin L., 1960, *Wave Propagation and Group Velocity*, (New York and London, Academic Press).

[10] Stevens T.E.,Wahlstrand J.K., J. Kuhl and Merlin R., 2001, Science, 291, 627 (January 26, 2001)

[11] Jackson J.D., 1975, *Classical Electrodynamics*, (New York, Wiley).

[12] Smith G.S., 1992, Amer.J.Phys., 61, 147.

[13] Frank I.M., In the book: "To the memory of S.I.Vavilov",pp.172-192 (Izdat. AN SSSR, Moscow, 1953), in Russian.

[14] Frank I.M., Usp.Fiz.Nauk, 144, 251 (1984).

[15] Afanasiev G.N., Stepanovsky Yu.P.,2000, Physica Scripta, 61, 704

[16] Tamm I.E., 1939, J.Phys. USSR, 1, 439.

[17] Kobzev A,P, and Frank I.M., 1981, Yad. Phys. 34, 125

[18] Zrelov V.P., Lupiltsev V.P., Ruzicka J., 1988 NIM A270, 62.

[19] Afanasiev G.N., Kartavenko V.G. and Ruzicka J,, 2000, J. Phys. A, 32, 7585;

[20] Afanasiev G.N., Shilov V.M., 2000, J. Phys.D, 33, 2931.

Received by Publishing Department
on October 1, 2001.

Афанасьев Г.Н., Картавенко В.Г., Ружичка Я. Е2-2001-206
Особенности черенковского излучения в средах с дисперсией

Ранее полученные пространственно-временные распределения излучения, возникающего при равномерном движении заряда в веществе с дисперсией, применены к физически совершенно различным веществам (иодин и ZnSe), для которых существуют литературные данные по параметризации диэлектрической проницаемости. Для иодина резонансная частота лежит в ультрафиолетовой области, а для ZnSe — в инфракрасной. Представлены как аналитические формулы, так и численные расчеты для спектрального состава этого излучения. Оказывается, что для иодина имеется только одна критическая скорость, выше и ниже которой движущийся заряд излучает по-разному. Для ZnSe таких скоростей — две. Также исследуются осложнения, возникающие при измерении излучения от точечного заряда, равномерно движущегося в среде, ниже черенковского порога. По-видимому, эти соображения применимы к недавнему эксперименту, в котором наблюдалось подпороговое излучение электрических диполей, движущихся в ZnSe. Указаны альтернативные причины появления этого излучения.

Работа выполнена в Лаборатории теоретической физики им. Н.Н.Боголюбова ОИЯИ.

Препринт Объединенного института ядерных исследований. Дубна, 2001

Afanasiev G.N., Kartavenko V.G., Ruzicka J. E2-2001-206
Peculiarities of Cherenkov Radiation in Dispersive Media

Previously obtained space-time distributions of the radiation generated by a charge uniformly moving in medium with dispersion are applied to concrete substances with quite different physical properties (iodine and ZnSe) for which the parametrizations of dielectric permittivity are known from physical literature. For iodine, the resonance frequency lies in a far ultraviolet region, while for ZnSe it is in a far infrared. Both analytical and numerical spectral distributions corresponding to this radiation are obtained. It turns out that for iodine there is only one critical velocity below and above of which the moving charge radiates in a quite different way. There are two critical velocity for ZnSe. We discuss possible complications arising when the radiation of the point-like charge is measured below the Cherenkov threshold. Probably, these considerations are applicable to the recent experiment in which the radiation of electric dipoles below the Cherenkov threshold was observed. The alternative reasons for the appearance of this under-threshold radiation are pointed out.

The investigation has been performed at the Bogoliubov Laboratory of Theoretical Physics, JINR.

Preprint of the Joint Institute for Nuclear Research. Dubna, 2001

Макет Т.Е.Попеко

Подписано в печать 14.11.2001
Формат 60 × 90/16. Офсетная печать. Уч.-изд. л. 2,3
Тираж 425. Заказ 52953. Цена 2 р. 50 к.

Издательский отдел Объединенного института ядерных исследований
Дубна Московской области